American Mineralogist, Volume 68, pages 731–741, 1983

The extraction–quench technique for determination of the thermodynamic properties of solute complexes: application to quartz solubility in fluid mixtures

JOHN V. WALTHER

Department of Geological Sciences
Northwestern University, Evanston, Illinois 60201

AND PHILIP M. ORVILLE[1]

Department of Geology and Geophysics
Yale University, New Haven, Connecticut 06511

Abstract

A procedure is outlined that allows determination of the hydration state, charge and chemical stoichiometry, as well as the apparent standard molal Gibbs free energy of formation, of aqueous species from solubility measurements in fluid mixtures. Also described is a hydrothermal apparatus capable of obtaining the necessary solubility data in fluid mixtures. The apparatus was used to determine quartz solubilities in supercritical CO_2–H_2O and Ar–H_2O mixtures. Results of this investigation along with other values reported in the literature are consistent with a stoichiometry of the dominant aqueous silica species of $Si(OH)_4 \cdot 2H_2O$ in the supercritical region of H_2O. Knowledge of the hydration number of aqueous silica was used to predict silica concentrations in CO_2–H_2O mixtures in the system CaO–MgO–SiO_2–HCl–CO_2–H_2O at 2 kbar and 450°C.

Introduction

Our knowledge of the equilibrium states of crustal rock systems has increased enormously over the last 25 years. The power, but also a limitation, of the phase equilibrium approach to metamorphic petrology is that the end state is independent of the particular path followed to reach that state. Development of textures, mineral segregations and styles of deformation are all aspects of metamorphism and metamorphic rocks that are sensitive to rates of competing processes and, if they can be interpreted, provide information on the particular path followed to reach a given final state.

A volatile-rich electrolyte solution phase plays an important role in the metasomatic, recrystallization and deformation processes. Although the amount of intergranular fluid present in a rock at any instant may be very small, the total amount of fluid that has passed through a given volume of rock may be large (*e.g.*, Norton and Knight, 1977; Ferry, 1978; Walther and Orville, 1982). Chemical communication between separate grains and separate volumes of rock, if it occurs, is by way of reaction between crystal and fluid and then diffusion or flow transport of various constituents. Recent theoretical, experimental, and observational investigations (Carmichael, 1979; Dibble and Tiller, 1981; Rimstidt and Barnes, 1980; Schott *et al.*, 1981; Aagaard and Helgeson, 1982, and others) suggest that near equilibrium the chemical affinity per effective surface area of mineral dissolution into the fluid phase is the rate controlling step in metasomatic processes. Quantitative modeling of rates and transport processes, therefore, requires values for the thermodynamic properties of the fluid phase, identification of the major species present in solution and thermodynamic data for these solution species.

One of the most successful experimental techniques used to obtain thermodynamic data on aqueous species was that pioneered by H. P. Eugster and his coworkers (*e.g.*, Eugster and Skippen, 1967; Frantz and Eugster, 1973; Crerar *et al.*, 1978; Gunter and Eugster, 1978; Frantz *et al.*, 1981). The technique involves the buffering of fugacities of both volatile and nonvolatile species by employing solid phases + H_2O as buffers to control oxygen, hydrogen, and chloride in solution within a sealed noble metal capsule. In this technique as well as others that employ sealed capsules in conventional cold seal reaction vessels, the experimental charge is quenched by water or compressed air at the end of an experimental run. After quench the capsules are opened and the concentration of solutes determined. Numerous problems can occur because minerals and solutions remain in contact during the quench. When extremely low solubilities are measured even very minor reactions between solution and the primary solid phases on quench

[1] Died April 2, 1980.

0003–004X/83/0708–0731$02.00

may significantly change the relative concentration of cations from those present in solution at high pressure and temperature. Recent efforts in experimental design have attempted to shorten the time of the quench process and thus diminish quench effect problems.

More recently Dickson and coworkers (Dickson *et al.*, 1963; Ryuba and Dickson, 1974; Seyfried *et al.*, 1979) have developed a large volume gold bag reaction cell. A single capillary exit tube allows extraction of fluid at constant pressure and temperature. Present designs permit the reaction cell to operate at pressures to 1 kbar and temperature to 500°C. Because fluid is separated from solid phases at the pressure and temperature of the experiment, back reactions between fluid and primary phases on quenching are eliminated. This reaction cell has been used extensively for investigations of seawater–rock interactions (*e.g.*, Bischoff and Dickson, 1975; Bischoff and Seyfried, 1978; Seyfried and Dibble, 1980; Seyfried and Bischoff, 1981; Shanks *et al.*, 1981; Seyfried and Mottl, 1982).

In this communication we describe an extraction-quench apparatus which also samples fluid separated from the solid phases at the pressure and temperature of the experiment. Because both volatiles and nonvolatile constituents are measured directly from the fluid sample after extraction, solution buffers need not be used. Ambiguities arising from uncertainties in fluid composition induced by buffering assemblages can therefore be eliminated. The apparatus allows equilibrium to be approached from either the supersaturated or undersaturated state. Solubility experiments can be designed to obtain the hydration state, charge and chemical stoichiometry of aqueous species. The extraction-quench apparatus was used to measure quartz solubilities in H_2O, H_2O-argon and H_2O–CO_2 mixtures from which the hydration state of aqueous silica was determined.

Determination of the stoichiometry of aqueous species from solubility measurements

At constant chemical potential of an anhydrous oxide constituent, the concentration of the dominant species will depend upon the activities of all other solution species which combine with the anhydrous oxide to form the particular hydrated species, whether a neutral or charged complex and whether associated or fully dissociated. For a given cation, the dominant species in solution may well be different in pure water from the present in a chloride-bearing electrolyte solution or in an H_2O–CO_2 mixture and, for a given solvent, the dominant species may change with pressure and temperature.

Solution of a simple crystalline anhydrous oxide of cation A in H_2O to form a hydrated complex can be represented by the reaction:

$$AO_{z_A/2} + m_{H^+}H^+ \cdot \mathbf{n}_{H^+}H_2O + \Delta\mathbf{n}H_2O \rightleftarrows AO_{z_A/2} \cdot m_{H^+}H^+ \cdot \mathbf{n}_cH_2O \quad (1)$$

where z_A is the ionic charge of cation A, m_{H^+} is the number of protons (H^+) added to the complex, $\mathbf{n}_{H^+}$ is the number of H_2O molecules coordinated in each proton complex, $\mathbf{n}_c$ is the number of H_2O molecules in the A-bearing complex (hydration number) and $\Delta\mathbf{n} = \mathbf{n}_c - m_{H^+}\mathbf{n}_{H^+}$.

An equilibrium constant at elevated temperature and pressure, $K_{T,P}$, for Reaction (1) is given by

$$K_{T,P} = \frac{a_{\text{A-complex}}}{a_{\text{A-oxide}} a_{H^+}^{m_{H^+}} a_{H_2O}^{\Delta n}} \quad (2)$$

where a is the activity of the subscripted species relative to an appropriate standard state with A-complex and A-oxide formulated as in Reaction (1).

If the standard state for A-oxide is defined as the simple oxide at pressure and temperature the equilibrium constant for the formation of A-complex from the simple oxide is:

$$K_{T,P} = \frac{a_{\text{A-complex}}}{a_{H^+}^{m_{H^+}} a_{H_2O}^{\Delta n}}. \quad (3)$$

If A-complex is the dominant A-containing complex in the solution, then Equation (3) gives a close approximation to the equilibrium solubility constant for the oxide compound at a particular temperature and pressure which is essentially pure H_2O reduces to

$$K_{T,P} = \frac{\gamma_{\text{A-complex}} m_{\text{A-complex}}}{a_{H^+}^{m_{H^+}}} \quad (4)$$

if pure H_2O liquid at P and T is taken as the standard state of H_2O. $\gamma_{\text{A-complex}}$ and $m_{\text{A-complex}}$ are the individual activity coefficient and molal concentration of the A-complex, respectively. The value of m_{H^+} will be positive if the complex is positively charged, negative if the complex is negatively charged, and zero if the complex is neutral.

From Equation 4 we can write

$$\Delta G^\circ_{P,T,\text{A-complex}} = \frac{-2.303RT}{a_{H^+}^{m_{H^+}}} \log \gamma_{\text{A-complex}} m_{\text{A-complex}} + \Delta G^\circ_{P,T,\text{A-oxide}} \quad (5)$$

where R refers to the gas constant, T is the temperature in K, and $\Delta G^\circ_{P,T,\text{A-oxide}}$ and $\Delta G^\circ_{P,T,\text{A-complex}}$ designate the apparent standard molal Gibbs free energy of formation of the subscripted species, which is defined by Benson (1968) and Helgeson and Kirkham (1976) as

$$\Delta G^\circ_{P,T,\text{A-oxide}} \equiv \Delta G^\circ_{f,Pr,Tr,\text{A-oxide}} + (G^\circ_{P,T,\text{A-oxide}} - G^\circ_{Pr,Tr,\text{A-oxide}}) \quad (6)$$

and

$$\Delta G^\circ_{P,T,\text{A-complex}} \equiv \Delta G^\circ_{f,Pr,Tr,\text{A-complex}} + (G^\circ_{P,T,\text{A-complex}} - G^\circ_{Pr,Tr,\text{A-complex}}) \quad (7)$$

The parenthetical terms in Equations (6) and (7) represent the difference in the standard molal Gibbs free energies of the species arising from an increase in pressure and temperature from Pr, Tr to P, T, and $\Delta G^\circ_{f,Pr,Tr,A\text{-oxide}}$ and $\Delta G^\circ_{f,Pr,Tr,A\text{-complex}}$ stand for the standard molal Gibbs free energies of formation from the elements of the subscripted species at Pr, Tr. If $a_{H^+}^{m_{H^+}}$ can be calculated (from knowledge of the pH of the solution) and $\gamma_{A\text{-complex}}$ estimated (Helgeson, Kirkham and Flowers, 1981), $\Delta G^\circ_{P,T,A\text{-complex}}$ can be calculated from Equation (5) and knowledge of the value of $\Delta G^\circ_{P,T,A\text{-oxide}}$.

The derivative of the logarithm of Equation (4) can be written as

$$\mathrm{d}(\log K_{T,P}) = 0 = \mathrm{d}(\log \gamma_{A\text{-complex}}) + \mathrm{d}(\log m_{A\text{-complex}}) - m_{H^+}\mathrm{d}(\log a_{H^+}) \quad (8)$$

If $\gamma_{A\text{-complex}}$ remains nearly constant under the conditions of the experiments, then the relationship between solubility and H^+ ion activity is given by:

$$\mathrm{d}(\log m_{A\text{-complex}}) \simeq m_{H^+}\mathrm{d}(\log a_{H^+}) \quad (9)$$

For small changes in H^+ ion activity, solubility which varies directly with H^+ ion activity indicates a positively charged complex, solubility which varies inversely with H^+ ion activity indicates a negatively charged complex, and solubility which is indifferent to H^+ ion activity indicates a neutral complex. If the dominant cation complex is a neutral species, Equation (3) reduces to:

$$K_{T,P} = \frac{a_{A\text{-complex}}}{a_{H_2O}^{\mathbf{n}_c}} = \frac{\gamma_{A\text{-complex}}\, m_{A\text{-complex}}}{a_{H_2O}^{\mathbf{n}_c}} \quad (10)$$

and if $a_{A\text{-complex}}$ is directly proportional to $m_{A\text{-complex}}$, molality of the A-complex in the solution, then solubility of the oxide phase as expressed in molality will vary with activity of H_2O as indicated in Equation (11) below.

$$\frac{\mathrm{d}\log m_{A\text{-complex}}}{\mathrm{d}\log a_{H_2O}} \simeq \mathbf{n}_c. \quad (11)$$

A series of solubility experiments at constant T and P but variable a_{H_2O} in which the same neutral hydrated complex is dominant, would therefore allow $\mathbf{n}_c$, the hydration number of the A-bearing complex, to be determined.

The activity of H_2O in the solution can be varied by mixing with another volatile, for example Ar or CO_2, whose mixing properties with H_2O have been determined experimentally or can be predicted theoretically. It is essential that the diluent volatile not react with either the oxide phase or the hydrated complex in solution over the range of mixtures studied experimentally.

If the dominant hydrated complex in solution in equilibrium with the oxide phase is a charged species, then from Equation (3) at constant T and P we can derive:

$$\frac{\mathrm{d}\log a_{A\text{-complex}}}{\mathrm{d}\log a_{H_2O}} = m_{H^+}\frac{\mathrm{d}\log a_{H^+}}{\mathrm{d}\log a_{H_2O}} + \Delta\mathbf{n}. \quad (12)$$

The term $\Delta\mathbf{n}$ is not the hydration number of the complex but is instead the difference between $\mathbf{n}_c$, the hydration number of the complex, and $m_{H^+}\mathbf{n}_{H^+}$, the total number of H_2O molecules complexed with protons which are consumed to make a positive charged complex (m_{H^+} positive) or released to make a negative charged complex (m_{H^+} negative).

From Equation (12) it can be seen that the change in solubility of the simple oxide phase at constant pressure and temperature is not only a function of a_{H_2O} but also of a_{H^+} where a charged species is dominant. Quite different results might be expected for CO_2 and Ar as diluents of H_2O because CO_2 forms partially ionized complexes with H_2O whereas Ar does not.

The consistency of $\gamma_{A\text{-complex}}$ over a range of concentrations of the dominant hydrated complex could be demonstrated by determining that the concentration of the cation in hydrous solutions in equilibrium with different solid phase assemblages at the same pressure and temperature varies directly with activity of the simple oxide component in the solid phase assemblage, so that

$$\Delta \log m_{A\text{-complex}} = \Delta \log a_{A\text{-oxide}}. \quad (13)$$

Equations (1) and (2) can be generalized to allow for formation of a dominant cation complex which contains chloride or other anions, CO_2, and alkali cations.

Extraction quench apparatus

Figure 1 shows the arrangement of the experimental apparatus used in this study. The reaction vessel is a relatively large volume (~35 cm^3) Morey-type vessel capable of work to 750°C and 4 kbar machined from a nickel–chromium–cobalt alloy (RENÉ 41). Greenwood (1961) has used a somewhat similar vessel of smaller charge volume to perform P–V–T measurements of Ar–H_2O mixtures. Closure of the reaction vessel is by way of a copper washer Bridgeman seal between the closure piece (also RENÉ 41) and the reaction vessel. The initial seal is made by tightening the hexagonal headed main nut onto a driving washer which compresses the copper washer. The opening on the reaction vessel is tapered outward 2½° to facilitate removal of the copper washer and closure piece.

Three 316 stainless steel capillary tubes (I.D. = 0.006 inches) enter the reaction vessel through a hole in the closure piece. These are sealed by driving a 3-hole 316 stainless steel tapered plug into the closure piece on the high pressure end and brazing capillaries, plug and closure piece together with Au–Ni brazing compound (see Fig. 2). Temperature within the charge volume is monitored by three thermocouples inserted in holes along the charge volume which are connected to a digital readout millivolt meter. The thermocouples were calibrated against a standard thermocouple which was calibrated against the melting points of cesium chloride and sodium chloride. Temperature was controlled by a voltage proportional controller connected to a platinum resistance

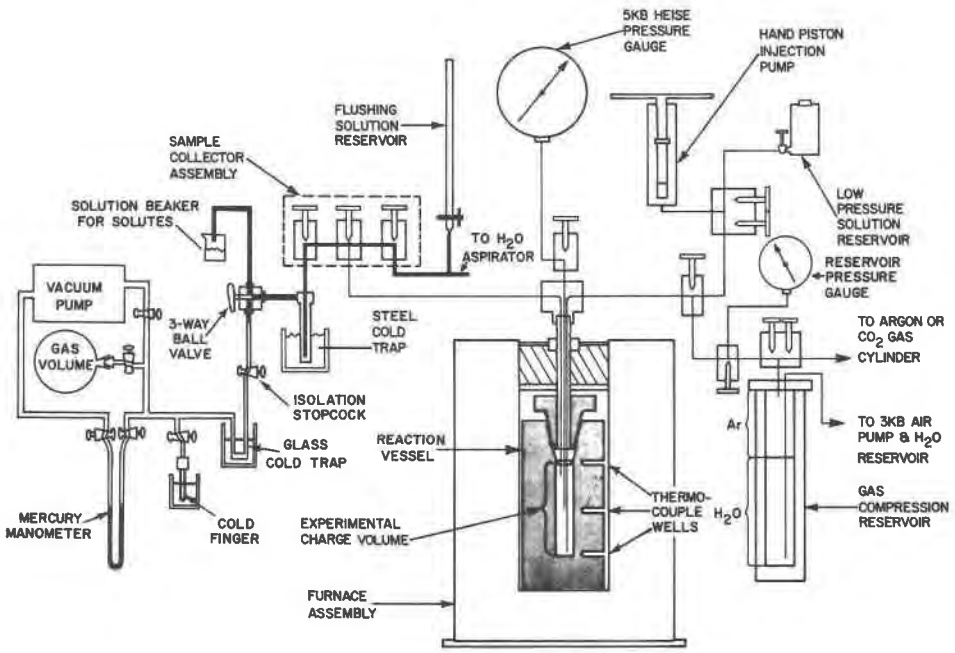

Fig. 1. Experimental apparatus for determination of solubilities in fluid mixtures.

thermometer inserted between the furnace coils and insulation. Temperature gradients along the sample volume were 3°C or less. Temperatures are probably accurate to within ±5°C. Pressure is measured with a Heise gauge connected to one of the capillary tubes. Uncertainty in the pressure reading was about 10 bars.

H_2O solutions, CO_2 or Ar are injected into the charge volume by use of a hand driven piston injector or from a gas compression reservoir as shown in Figure 1.

Before sampling, the sample collector assembly, gas volume, cold traps and finger and the interconnected tubing are evacuated with the aid of the vacuum pump. When evacuation is completed the vacuum pump is isolated from the extraction apparatus by closing the two stopcocks that connect it to the apparatus. The charge volume is sampled for ~5 seconds. The volume of the sample collector which consists of the volume within the valve blocks and the ¼" O.D. stainless steel tubing between blocks was ~0.9 cm^3 in this study.

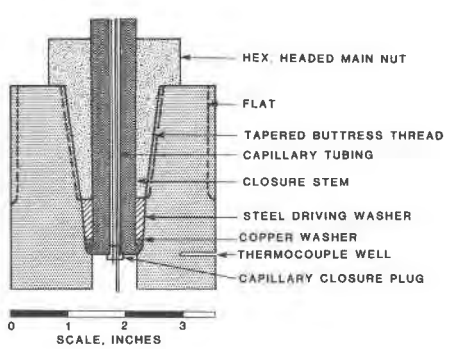

Fig. 2. Configuration of closure pieces in the reaction vessel.

The steel cold trap is immersed in liquid nitrogen. Stopcocks are opened so that gas may pass freely from the steel cold trap to the gas volume and manometer. The sample collector valve that is connected to the steel cold trap is opened slowly. The condensable fluid (H_2O solution) is frozen in the steel cold trap while most of the argon passes through the system into the gas volume. When using CO_2 rather than Ar, a slush of solid CO_2 and 2-Butoxyethenol is used to freeze the H_2O solution and allow passage of CO_2. After pressure throughout the apparatus has stabilized the isolation stopcock is closed. The temperature of the argon is then allowed to stabilize. The argon pressure is measured on the monometer and the temperature measured by a thermometer adjacent to the gas volume. The system to the isolation stopcock is again evacuated and the isolation stopcock is opened to release much of the remaining argon into the gas volume where it is again measured. This procedure is repeated until all detectable argon is measured and evacuated from the apparatus (generally three measurements). The volume of the system used in the Ar (or CO_2) measurement includes glass tubing between isolation stopcock and gas volume, the gas volume itself, and the volume added by the manometer. The total volume of the system was ~1210 cm^3, of which the gas volume contributed 89%. Knowledge of the volume of Ar (or CO_2) and its pressure and temperature allowed calculation of its mass by use of the data of Hilsenrath *et al.* (1955).

Table 1. Experimental results for quartz solubility in H_2O. The numbered sequence indicates the order in which the measurements were done. The duration time is the time at which the new pressure and/or temperature was maintained before sampling. The starting conditions for a given measurement are, therefore, given by the previous measurement. The starting composition is modified somewhat by H_2O introduced between samples to bring the charge volume to the desired pressure at the new temperature.

Sample	Pressure (bars)	Temperature (°C)	Duration (days)	Log Molality SiO_2(aq)
B-1	2000	400	5	-1.392
B-2	2000	400	2	-1.394
B-3	2000	400	2	-1.389
B-4	2000	425	5	-1.320
B-5	2000	450	5	-1.235
B-6	2000	450	2	-1.251
B-7	2000	475	5	-1.202
B-8	2000	500	5	-1.158
B-9	2000	500	3	-1.145
B-10	2000	525	4	-1.077
B-11	2000	525	2	-1.108
B-12	2000	525	2	-1.084
B-13	2000	525	2	-1.098
B-14	2000	550	5	-1.055
B-15	1000	550	5	-1.356
B-16	1000	500	5	-1.387
B-17	1000	460	5	-1.404
B-18	1000	400	5	-1.543
B-19	1000	350	5	-1.656
B-20	2000	350	4	-1.515

After the argon measurement the glass cold trap is immersed in a liquid nitrogen bath. The isolation stopcock is opened and the steel cold trap heated with a forced air heat gun. This continues until all the solid H_2O is sublimed and transferred to the glass cold trap where it is again frozen. The isolation stopcock is closed and H_2O is transferred to the cold finger by immersing the cold finger in liquid N_2 and heating the glass cold trap with the forced air heat gun. When all the H_2O is transferred the cold finger is detached, sealed with a rubber stopper, allowed to come to room temperature, and weighed. The mass of H_2O within the cold finger is then determined by weight difference. Reproducibility of the mass of H_2O measured by this procedure was found to be within ± 0.01 gm.

It is assumed that no solutes are transferred beyond the steel cold trap by this procedure. (In quartz solubility experiments no silica was detected in the H_2O transferred to the cold finger.) After removal of H_2O by the procedure outlined above, the solutes are collected by passing a flushing solution that is able to dissolve them from the flushing solution reservoir through the sample collector assembly and steel cold trap by turning the 3-way ball valve and collecting solute and flushing solution in a telfon beaker (see Fig. 1). In the case of silica a 0.7 wt.% NaOH solution was used. Typically the flushing solution is allowed to stand overnight in the apparatus to insure the removal of the solutes. It should be noted that between the sample collector and solution beaker the solution is in contact with 316 stainless steel and teflon only. The solutions are stored in air tight plastic bottles until analysis. The absolute moles of solute can be determined by knowledge of the weight of the collected flushing solution and measurement of the solute concentration within the flushing solution. After the sample is collected the path of the flushing solution is rinsed with distilled, deionized water and dried with an H_2O aspirator. No error is thought to be introduced because of the $<1\%$ volume of fluid included in the sample from the sampling capillary. If this problem is of concern, repeated sampling at identical pressure and temperature should minimize its effects.

Quartz solubilities in pure H_2O

Optically clear natural quartz of grain size greater than 100 mesh was loaded along with deionized, distilled, decarbonated water into the reaction vessel. The main nut was tightened to produce an initial seal with the copper washer. The reaction vessel was brought to pressure and temperature. Solution was bled from the vessel through the collector assembly to adjust the pressure. Any silica deposited by this procedure was leached from the apparatus by passing 0.7 wt.% NaOH and then distilled, deionized water through the collector assembly before sampling. Samples were acidified shortly before analysis. Silica concentrations were determined by the molybdate blue method as outlined by Strickland and Parsons (1965). Duplicate analyses were performed on all samples and routinely gave silica concentrations with an agreement of 1% or better.

The results of these experiments are given in Table 1 and plotted in Figure 3. Examination of Figure 3 reveals the excellent agreement between the results reported here

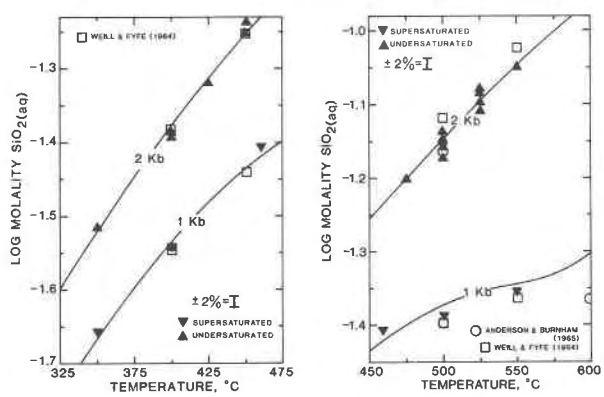

Fig. 3. Experimental results for quartz solubility in pure H_2O obtained between 350° and 550°C at 1 and 2 kbar. Upward or downward pointing triangles indicate equilibria approached from an undersaturated or supersaturated state, respectively.

and other investigations using standard cold seal reaction vessels. The solid lines in Figure 3 were computed from equations for quartz solubility given by Walther and Helgeson (1977). The excellent agreement confirms that the experimental apparatus and procedure gives reliable results at least in the pressure and temperature regions shown in Figure 3.

Hydration number of aqueous silica

The nature of aqueous silica hydration in aqueous solutions has been the subject of considerable discussion (Wendlandt and Glemser, 1963; Weill and Fyfe, 1964; Weill and Bottinga, 1970; Anderson and Burnham, 1965; Sommerfeld, 1967; Crerar and Anderson, 1971; Novgorodov, 1975; Shettel, 1974; Walther and Helgeson, 1977, 1980; Marshall, 1980). Explicit representation of solvation of aqueous silica in quartz solubility reactions can be written

$$SiO_{2(qtz)} + \mathbf{n}H_2O \rightleftarrows SiO_2 \cdot \mathbf{n}H_2O \qquad (14)$$

where $SiO_{2(qtz)}$ represents quartz, $SiO_2 \cdot \mathbf{n}H_2O$ stands for the predominant uncharged but solvated silica species in solution and **n** denotes the hydration number of the silica species. Assuming the activity coefficient of the aqueous silica species is unity (see Walther and Helgeson, 1977 for discussion), Equation (11) written for Reaction (14) is:

$$\frac{\mathrm{d} \log m_{SiO_2 \cdot \mathbf{n}H_2O}}{\mathrm{d} \log a_{H_2O}} = \mathbf{n} \qquad (15)$$

where $m_{SiO_2 \cdot \mathbf{n}H_2O}$ is the molality of the dominat hydrated silica species, and a_{H_2O} stands for the activity of H_2O. Therefore, **n** is given by the slope of the line connecting experimental determinations in plots of log $m_{SiO_2 \cdot \mathbf{n}H_2O}$ against log a_{H_2O} at constant pressure and temperature. It is assumed that the same dominant silica species is stable throughout the range of fluid mixing. It should be noted that any effects of interaction between the aqueous silica species and the fluid on the activity of the hydrated silica species are also incorporated into the value of **n**.

Reduction of activity of H_2O can be accomplished by mixing with CO_2 because silica solubility in CO_2 is below detection under the temperature and pressure region in this study. CO_2 is assumed to display no significant interaction with the hydrated silica species. Unfortunately, there is considerable disagreement among investigators as to the supercritical mixing properties of CO_2 and H_2O (Holloway, 1977; Flowers, 1979; Kerrick and Jacobs, 1981; Greenwood, 1973). While it is generally agreed there is positive deviation from ideal mixing of CO_2–H_2O, the magnitude of the deviation is in question.

Figure 4 shows plots of log $m_{SiO_{2(aq)}}$ against log X_{H_2O} for quartz solubilities in CO_2–H_2O mixtures from the work of Shettel (1974) and Novogordov (1975). Values obtained in the present study at 600°C and 2 kbar are also shown in Figure 4 as well as tabulated in Table 2. The 600°C and 2 kbar determinations were approached from the supersaturated state.

Mole fraction of H_2O rather than activity was used because of the uncertainties in the mixing properties of CO_2–H_2O. If CO_2–H_2O mixed ideally the activity of H_2O would be identical to mole fraction. The end points of arrows show the shift in position of the connected symbol if the abscissa is changed to log a_{H_2O} and the mixing properties of CO_2–H_2O reported by Kerrick and Jacobs (1981) are used. Smaller shifts of the symbol would result if the mixing equations of Flowers (1979) were used. While all determinations will shift at least slightly if plotted against log a_{H_2O} rather than log X_{H_2O}, only the shifts of some representative determinations are shown to increase the clarity of presentation. Because of the low concentration of aqueous silica in solution the a_{H_2O} is assumed to be only a function of mixing along the silica free CO_2–H_2O binary. Therefore differences between log a_{H_2O} and log X_{H_2O} will be similar at similar values of log X_{H_2O} at constant pressure and temperature. Additionally, the departure of log a_{H_2O} from that of ideal mixing increases as X_{H_2O} decreases. Very little shift occurs for the H_2O rich determinations (less than 0.01 at log $X_{H_2O} = -0.05$ for the pressures and temperatures shown in Fig. 4) but large shifts occur with CO_2 rich fluid mixtures if the abscissas in Figure 3 are changed to log a_{H_2O}.

Inspection of Figure 4 reveals that within experimental uncertainty $\mathbf{n} = 4$ for the pressures and temperatures studied in the various investigations. Only Novgorodov's (1975) work at 3 kbar and 700°C appears inconsistent with $\mathbf{n} = 4$, particularly at low X_{H_2O}. It is not clear what is responsible for the behavior as investigations at both 2 kbar and 5 kbar at 700°C are consistent with $\mathbf{n} = 4$. The data of Novgorodov (1975) indicate that the hydration number of silica decreases at low values of X_{H_2O}. This implies that there may be significant interaction between CO_2 and the aqueous silica complex at low X_{H_2O} or that H_2O–CO_2 mixtures display a much greater degree of nonideality than that computed by Kerrick and Jacobs (1981).

Strictly speaking, log $m_{SiO_2 \cdot \mathbf{n}H_2O}$ should be used in constructing the plots in Figure 4. Because the molality of silica in solution is low, the number of waters of hydration

Table 2. Experimental results for quartz solubility at 2 kbar and 600°C in CO_2–H_2O mixtures

Sample	Duration (days)	Moles Ar x 10^2	Moles H_2O x 10^2	log $m_{SiO_{2(aq)}}$	X_{H_2O}
W-1	4	0.102	4.45	-0.964	0.977
W-2	2	0.158	4.39	-1.017	0.964
W-3	2	0.394	3.98	-1.112	0.901
W-4	3	0.404	3.64	-1.125	0.889
W-5	2	0.533	3.27	-1.201	0.837
W-6	2	0.718	2.41	-1.429	0.702
W-7	2	0.734	2.36	-1.513	0.689

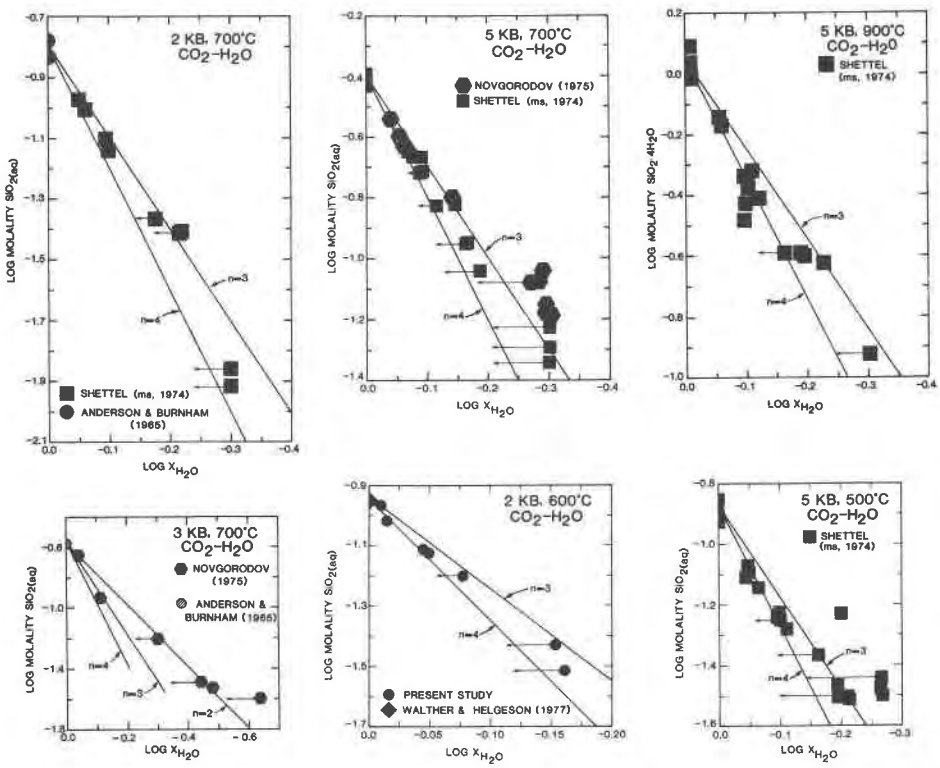

Fig. 4. Constant pressure and temperature plots for quartz solubility determinations in CO_2–H_2O mixtures for a variety of pressures and temperatures. Endpoint of arrows show, for representative points, the shift of the connected point if the abscissa is changed to log activity of H_2O (see text). Lines marked n = 2, 3, or 4 give the predicted solubility behavior for these hydration states of aqueous silica.

that need to be accounted for in addition to the 55.51 moles of H_2O in the molality calculation generally has no significant effect. With **n** = 4, concentrations of log $m_{SiO_{2(aq)}} \leq -0.4$ will effect molality calculations by less than 3%. The 900°C and 5 kbar determinations exceed this value and were, therefore, plotted against log $m_{Si(OH)_4 \cdot 2H_2O}$.

Shettel's detailed study (1974) using a similar approach found hydration numbers of 4.4 (2 kbar and 700°C), 4.6 (5 kbar and 500°C), 4.6 (5 kbar and 700°C), and 5.3 (5 kbar and 900°C). He cast Equation (15) in terms of mole fraction of the silica complex rather than molality as used in this study for his determination of the hydration number. Because mole fraction is not a linear function of molality, significant differences result in using Equation (15) with the two concentration scales at high silica concentrations. Use of mole fraction rather than molality results in higher calculated hydration numbers with the difference increasing with increasing silica concentration. This accounts, at least in part, for differences between Shettel's highest calculated hydration number (5.3) which was obtained in experiments where the concentration of silica in solution was high and 4.0 found in this study. More consistent hydration numbers result if the molality concentration scale is used.

The results of quartz solubility experiments in Ar–H_2O mixtures by Sommerfeld (1967) and those determined in the present study are shown in Figure 5 for 1 kbar at 400° and 500°C. As discussed previously, the shifts shown by the endpoints of the arrows are those computed for representative determinations if the abscissas are

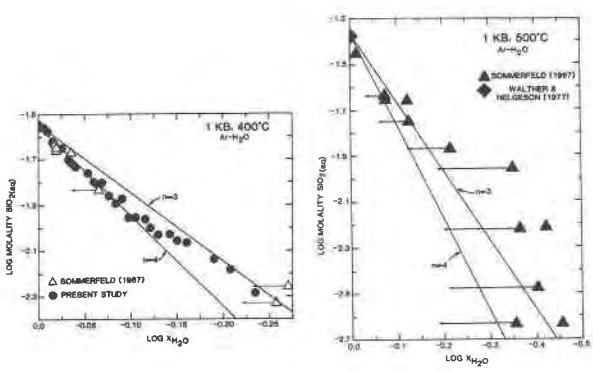

Fig. 5. Plots of log molality of SiO_2(aq) versus log mole fraction of H_2O for quartz solubility measurements in Ar–H_2O mixtures at 1 kbar and 400° and 500°C. See caption of Fig. 4 for significance of arrows and lines marked n = 3 and n = 4.

Table 3. Experimental results for quartz solubility at 1 kbar and 400°C in Ar–H_2O mixtures

Sample	Duration (days)	Moles Ar x 10^2	Moles H_2O x 10^2	log $m_{SiO_2(aq)}$	X_{H_2O}
B-27B	2	0.000	5.22	-1.543	1.000
B-28	6	0.012	4.97	-1.559	0.998
B-29	3	0.047	4.70	-1.557	0.990
B-30	4	0.110	4.65	-1.572	0.977
B-31	2	0.168	4.60	-1.621	0.965
B-32	4	0.269	4.42	-1.648	0.943
B-33	1	0.335	4.35	-1.702	0.929
B-34	1	0.366	4.21	-1.716	0.920
B-35	2	0.432	3.83	-1.733	0.899
B-36	3	0.490	3.74	-1.758	0.884
B-37	2	0.558	3.69	-1.799	0.869
B-38	1	0.582	3.60	-1.824	0.861
B-39	2	0.594	3.51	-1.801	0.855
B-40	6	0.656	3.43	-1.863	0.840
B-41	3	0.708	3.34	-1.893	0.825
B-42	2	0.754	3.26	-1.872	0.812
B-43	2	0.796	3.18	-1.958	0.800
B-44	3	0.842	3.07	-1.951	0.785
B-45	2	0.894	2.92	-1.961	0.766
B-46	2	0.934	2.89	-1.999	0.756
B-47	3	0.967	2.78	-2.030	0.742
B-48	2	0.983	2.66	-2.026	0.719
B-49	2	1.041	2.53	-2.054	0.709
B-50	3	1.105	2.48	-2.063	0.692
B-51	2	1.284	2.33	-2.138	0.645
B-52	2	1.360	2.21	-2.181	0.619
B-53	2	1.478	2.07	-2.287	0.583

changed to log a_{H_2O}. The mixing properties of Ar–H_2O are those reported by Sommerfeld (1967) for 400°C and Greenwood (1961) for 500°C. Quartz solubilities at 400°C and 1 kbar determined in this study are also given in Table 3. All determinations from this study were approached from the supersaturated state.

Although $\mathbf{n} = 4$ is consistent with quartz solubility determinations at 500°C, a hydration number of 4 appears inconsistent with determinations at 400°C. Corrections for log X_{H_2O} between -0.05 and -0.19 would require hydration numbers of 8 or greater. We concude that the mixing properties of Ar–H_2O in this region as reported by Sommerfeld (1967) are in error and instead are much more nearly ideal. Because the corrections are taken from unpublished work of Sommerfeld's, no analysis of possible error could be undertaken.

It is widely assumed that the four-fold coordination of silicon with oxygen in mineral phases is preserved with hydroxyls in aqueous solution. Experimental investigations tend to confirm this assumption at least at 25°C (Lagerstrom, 1959; Engelhardt *et al.*, 1975). The dominant uncharged aqueous silicon species is therefore written as $Si(OH)_4$ implying a hydration number of 2. If in fact the hydration number of aqueous silicon is 4 and if aqueous silicon is tetrahedrally coordinated by hydroxyls, two more H_2O water dipoles must also be included in the aqueous species. Figure 6 shows a possible configuration of the silicate species where the silicon atom is tetrahedrally coordinated by hydroxyls and two additional water molecules are attached by hydrogen bonding. The hydrogens of the tetrahedral hydroxyls are shown shifted off the apices of the tetrahedron in order to avoid the hydrogens of the two water dipoles. As defined by Bockris (1949) the two water dipoles are included in the primary hydration of Si, that is, the hydrated silica complex, $Si(OH)_4 \cdot 2H_2O$, moves as one entity in solution.

Activity coefficients of H_2O in Ar–H_2O mixtures

Quartz solubility experiments at 2 kbar in a fixed composition of Ar–H_2O were performed between 402° and 618°C. The procedure consisted of bringing the experimental charge volume which included quartz crystals and an Ar–H_2O fluid with $X_{H_2O} = 0.82$ to 402°C and 2 kbar. After 2 days a sample was withdrawn and analyzed. After withdrawing the sample the charge volume temperature was increased until the pressure was again at 2 kbar. The results of these measurements are given in Table 4. The duration is the time the charge volume was held at the new temperature before sampling. The sample number indicates the order in which the sampling was done. All experiments were, therefore, approached from a state undersaturated with respect to quartz. Because no fluid was introduced between sampling the mole fraction of H_2O of all samples was considered constant. Inspection of Table 4 reveals that the precision of the X_{H_2O} measurement is 2% or better.

With knowledge of the hydration number of aqueous silica and assuming a unit coefficient for the aqueous silica complex γ_{H_2O}, the mole fraction activity coefficient of H_2O, can be computed by rearranging the mass action equation for Reaction (14):

$$\gamma_{H_2O} = \left[\frac{m_{Si(OH)_4 \cdot 2H_2O}}{K}\right]^{1/4} \cdot \frac{1}{X_{H_2O}} \qquad (16)$$

The results of this calculation are also shown in Table 4. The equilibrium constant, K, was computed from the equations given by Walther and Helgeson (1977). Uncertainty in the calculation is difficult to ascertain. The temperature and pressure and each of the quantities in

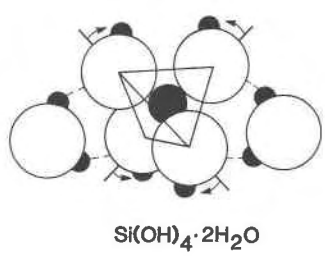

$Si(OH)_4 \cdot 2H_2O$

Fig. 6. Proposed configuration of the aqueous silica complex. The large solid circle represents the silicon atom, the large open circles oxygen atoms and the small solid circles hydrogen atoms. Four hyroxyls are shown tetrahedrally coordinated to the silicon atom with two water molecules attached by hydrogen bonding.

Table 4. Experimental results for quartz solubility at 2 kbar and $X_{H_2O} = 0.82$ in Ar–H_2O mixtures. Calculated values with relatively higher uncertainties are shown in parentheses.

Sample	Temp °C	Duration (days)	Moles Ar x 10^2	Moles H_2O x 10^2	log $m_{SiO_2(aq)}$	X_{H_2O}	Log K	γ_{H_2O}
C-2	402	2	0.822	3.49	-1.693	0.810	-1.365	1.02
C-3	431	2	0.780	3.63	-1.632	0.823	-1.292	1.00
C-4	461	2	0.780	3.65	-1.539	0.824	-1.222	1.01
C-5	489	3	0.778	3.65	-1.478	0.824	-1.162	1.01
C-6	517	2	0.757	3.65	-1.391	0.828	-1.105	1.02
C-7	549	2	0.767	3.66	-1.352	0.827	-1.043	1.01
C-8	583	3	0.764	3.64	-1.258	0.827	-0.967	1.02
C-9	618	5	0.808	3.61	-1.154	0.817	(-0.850)	(1.03)

Equation (16) is probably known to 3% or better. A conservative estimate of uncertainty of γ_{H_2O} is ±10% although the internal consistency appears better than this. Values of γ_{H_2O} computed from the *P–V–T* experiments of Greenwood (1961) on Ar–H_2O mixtures appear somewhat greater than those shown in Table 4. However, they are consistent within the stated experimental uncertainty.

Concluding remarks

Carefully designed solubility measurements of solid phases can be used to determine the stoichiometry and thermodynamic properties of solute species. The experimental apparatus and technique used in this investigation give reliable results as to the concentration of solutes in solution in equilibrium with a solid phase in fluid mixtures. Where contamination from either the René 41 or stainless steel may be a problem, gold plating of the charge volume and sample collection assembly and use of titanium tubing is recommended.

Analysis of quartz solubility data in CO_2–H_2O and Ar–H_2O mixtures indicates a solution species for aqueous silica with hydration number of 4 rather than 2 as is commonly assumed when writing the silica complex as H_4SiO_4 or $Si(OH)_4$. Similar decreases in quartz solubility as a function of a_{H_2O} occur in CO_2–H_2O and Ar–H_2O mixtures. It is proposed that the quartz solubility reaction, at least to values of X_{H_2O} as low as 0.5, is:

$$SiO_{2(qtz)} + 4H_2O \rightleftarrows Si(OH)_4 \cdot 2H_2O \qquad (16)$$

where $Si(OH)_4 \cdot 2H_2O$ is meant to imply a silicon with tetrahedrally coordinated hydroxyls and two additional H_2O water molecules attached by hydrogen bonding.

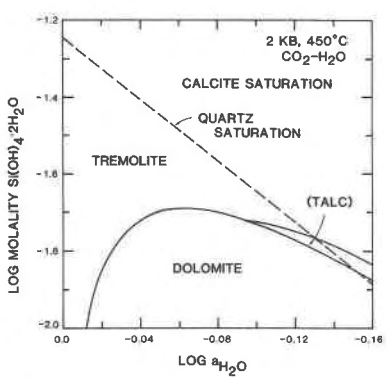

Fig. 7. Phase relations in the system CaO–MgO–SiO_2–HCl–CO_2–H_2O in the presence of calcite as a function of log $m_{Si(OH)_4 \cdot 2H_2O}$ and log a_{H_2O} at 2 kbar and 450°C.

Knowledge of the hydration number of aqueous silica allows prediction of the concentration of aqueous silica in fluid mixtures where a_{H_2O} departs from unity. Results can be applied to aqueous silica in solutions undersaturated with respect to quartz. Figure 7 shows an example at 2 kbar and 450°C in CO_2–H_2O mixtures for the system CaO–MgO–SiO_2–HCl–CO_2–H_2O calculated from the data given by Helgeson, Delany, Nesbitt, and Bird (1978) and Flowers (1979). Examination of Figure 7 reveals that in the presence of calcite, equilibrium between tremolite and dolomite requires the molality of silica in solution to first increase and then decrease as the activity of water decreases. Such behavior can not be anticipated without knowledge of the hydration number of aqueous silica (compare Fig. 23A of Walther and Helgeson, 1980).

Acknowledgments

K. V. Ragnarsdóttir determined the concentration of silica in many of the flushing solutions. The final experimental design and procedure benefited from discussion with D. Rye and F. Bishop. P. Merewether and A. Goodhue helped in the initial construction of the experimental apparatus. Thanks are also due to L. Steigely and C. Cheverton for typing and drafting. Critical reviews by J. Holloway and A. Navrotsky lead to substantial improvement of the manuscript. This work was supported by NSF grants EAR 79-04892 and EAR 80-24146. J. V. W. would like to acknowledge the encouragement, inspiration, and support of his coauthor, the

late Philip M. Orville, who introduced him to the ways of experimental petrology.

References

Aagaard, P. and Helgeson, H.C. (1982) Thermodynamic and kinetic constraints on reaction rates among minerals and aqueous solutions. I. Theoretical considerations. American Journal of Science, 282, 237–285.

Anderson, G. M. and Burnham, C. W. (1965) The solubility of quartz in supercritical water. American Journal of Science, 263, 494–511.

Benson, S. W. (1968) Thermochemical Kinetics. Wiley, New York.

Bischoff, J. L. and Dickson, F. W. (1975) Seawater-basalt interaction at 200°C and 500 bars: Implications for origin of sea-floor heavy-metal deposits and regulation of seawater chemistry. Earth and Planetary Science Letters, 25, 385–397.

Bischoff, J. L. and Seyfried, W. E., Jr. (1978) Hydrothermal chemistry of seawater from 25° to 350°C. American Journal of Science, 278, 838–860.

Bockris, J. O'M. (1949) Ionic Solutions. Chemical Society of London: Quarterly Reviews, 3, 173–180.

Carmichael, D. M. (1979) Some implications of metamorphic reaction mechanisms for geothermobarometry based on solid-solution equilibria. (abstr.) Geological Society of America, Abstracts with Programs, 11, 398.

Crerar, D. A. and Anderson, G. M. (1971) Solubility and solvation reactions of quartz in dilute hydrothermal solutions. Chemical Geology, 8, 107–122.

Crerar, D. A., Susak, N. J., Borcsik, M., and Schwartz, S. (1978) Solubility of the buffer assemblage pyrite + pyrrhotite + magnetite in NaCl solutions from 200 to 350°C. Geochimica et Cosmochimica Acta, 42, 1427–1437.

Dibble, W. E., Jr. and Tiller, W. A. (1981) Non-equilibrium water/rock interactions. I. Model for interface-controlled reactions. Geochimica et Cosmochimica Acta, 45, 79–92.

Dickson, F. W., Blount, C. W., and Tunell, G. (1963) Use of hydrothermal solution equipment to determine the solubility of anhydrite in water from 100° to 275° and from 1 bar to 1,000 bars pressure. American Journal of Science, 261, 61–78.

Engelhardt, G., Zeigan, D., Jancke, H., Hoebbel, D., and Wieker, W. (1975) Zur Abhängigkeit der Struktur der Silicataniomen in wässvigen Natriumsilicatlösungen vom Na:Si Verhältnis. Zeitschrift für Anorganische und Allgemeine Chemie, 418, 17–28.

Eugster, H. P. and Skippen, G. B. (1967) Igneous and metamorphic reactions involving gas equilibria. In P. H. Abelson, Ed., Researches in Geochemistry, Vol. 2, p. 377–396. Wiley, New York.

Ferry, J. M. (1978) Fluid interaction between granite and sediment metamorphism. American Journal of Science, 278, 1025–1056.

Flowers, G. C. (1979) Correction of Holloway's (1977) adaptation of the modified Redlich–Kwong equation of state for calculation of the fugacities of molecular species in supercritical fluids of geologic interest. Contributions to Mineralogy and Petrology, 69, 315–318.

Frantz, J. D. and Eugster, H. P. (1973) Acid-base buffers: use of Ag + AgCl in the experimental control of solution equilibria at elevated pressures and temperatures. American Journal of Science, 273, 268–286.

Frantz, J. D., Popp, R. K., and Boctor, N. Z. (1981) Mineral-solution equilibria. V. Solubilities of rock-forming minerals in supercritical fluids. Geochimica et Cosmochimica Acta, 45, 69–77.

Greenwood, H. J. (1961) The system $NaAlSi_2O_6$–H_2O–argon: Total pressure and water pressure in metamorphism. Journal of Geophysical Research, 66, 3923–3946.

Greenwood, H. J. (1973) Thermodynamic properties of gaseous mixtures of carbon dioxide and water between 0 and 500 bars. American Journal of Science, 273, 561–571.

Gunter, W. D. and Eugster, H. P. (1978) Wollastonite solubility and free energy of supercritical aqueous $CaCl_2$. Contributions to Mineralogy and Petrology, 66, 271–281.

Helgeson, H. C. and Kirkham, D. H. (1976) Theoretical prediction of the thermodynamic behavior of aqueous electrolytes at high pressures and temperatures: III. Equation of state for aqueous species at infinite dilution. American Journal of Science, 276, 97–240.

Helgeson, H. C., Delany, J. M., Nesbitt, H. W., and Bird, D. K. (1978) Summary and critique of the thermodynamic properties of minerals. American Journal of Science, 278A, 1–229.

Helgeson, H. C., Kirkham, D. H., and Flowers, G. C. (1981) Theoretical prediction of the thermodynamic behavior of aqueous electrolytes: IV. Calculation of activity coefficients, osmotic coefficients and apparent molal and standard and relative partial molal properties to 600°C and 5 kb. American Journal of Science, 281, 1249–1516.

Hilsenrath, J., Beckett, C. W., Benedict, W. S., Fano, L., Hoge, H. J., Masi, J. F., Nuttall, R. L., Touloukian, Y., and Woolley, H. W. (1955) Tables for thermal properties of gases. United States National Bureau of Standards, Circular 564.

Holloway, J. R. (1977) Fugacity and activity of molecular species in supercritical fluids, In D. G. Fraser, Ed., Thermodynamics in Geology, p. 161–181. Reidel, Dordrecht, The Netherlands.

Kerrick, D. M. and Jacobs, G. K. 1981) A modified Redlich–Kwong equation for H_2O, CO_2, and H_2O–CO_2 mixtures at elevated pressures and temperatures. American Journal of Science, 281, 735–767.

Lagerstrom, G. (1959) Equilibrium studies of polyanions: III. Silicate ions in $NaClO_4$ medium. Acta Chemica Scandinavica, 13, 722–736.

Marshall, W. L. (1980) Amorphous silica solubilities—III. activity coefficient relations and predictions of solubility behavior in salt solutions, 0–350°C. Geochimica et Cosmochimica Acta, 44, 925–931.

Norton, D. and Knight, J. (1977) Transport phenomena in hydrothermal systems: cooling plutons. American Journal of Science, 277, 937–981.

Novgorodov, P. G. (1975) Quartz solubility in H_2O–CO_2 mixtures at 700°C and pressures of 3 and 5 kbar. Geokhimica, no. 10, 1484–1489.

Rimstidt, J. D. and Barnes, H. L. (1980) The kinetics of silica-water reactions. Geochimica et Cosmochimica Acta, 44, 1683–1700.

Rytuba, J. J. and Dickson, F. W. (1974) Reaction of pyrite and pyrrhotite + quartz + gold with NaCl–H_2O solutions, 300–500°C, 500–1000 bars and genetic implications. Problems of Ore Deposition 4th IAGOD Symposium, Varna, Bolgaria, II, 320–326.

Schott, J., Berner, R. A., and Sjöberg, E. L. (1981) Mechanism of pyroxene and amphibole weathering: I. Experimental studies of iron-free minerals. Geochimica et Cosmochimica Acta, 45, 2123–2135.

Seyfried, W. E., Jr. and Bischoff, J. L. (1981) Experimental seawater-basalt interaction at 300°C, 500 bars, chemical exchange, secondary mineral formation and implications for the transport of heavy metals. Geochimica et Cosmochimica Acta, 45, 135–147.

Seyfried, W. E., Jr. and Dibble, W. E., Jr. (1980) Seawater-peridotite interaction at 300°C and 500 bars: implications for the origin of oceanic serpentinites. Geochimica et Cosmochimica Acta, 44, 309–321.

Seyfried, W. E., Jr., Gordon, P. C., and Dickson, F. W. (1979) A new reaction cell for hydrothermal solution equipment. American Mineralogist, 64, 646–649.

Seyfried, W. E., Jr. and Mottl, M. J. (1982) Hydrothermal alteration of basalt by seawater under seawater-dominated conditions. Geochimica et Cosmochimica Acta, 46, 985–1002.

Shanks, W. C., III, Bischoff, J. L., and Rosenbauer, R. J. (1981) Seawater sulfate reduction and sulfur isotope fractionation in basaltic systems: Interaction of seawater with fayalite and magnetite at 200–350°C. Geochimica et Cosmochimica Acta, 45, 1977–1995.

Shettel, D. L., Jr. (1974) The solubility of quartz in supercritical H_2O–CO_2 fluids. M.S. Thesis. Pennsylvania State University, University Park.

Sommerfeld, R. A. (1967) Quartz solution reaction: 400–500°C, 1000 bars. Journal of Geophysical Research, 72, 4253–5257.

Strickland, J. D. H. and Parsons, T. R. (1965) A Manual of Sea Water Analysis. Bulletin No. 125, Fisheries Research Board of Canada.

Walther, J. V. and Helgeson, H. C. (1977) Calculation of the thermodynamic properties of aqueous silica and the solubility of quartz and its polymorphs at high pressures and temperatures. American Journal of Science, 277, 1315–1351.

Walther, J. V. and Helgeson, H. C. (1980) Description and interpretation of metasomatic phase relations at high pressures and temperatures: I. Equilibrium activities of ionic species in nonideal mixtures of CO_2 and H_2O. American Journal of Science, 280, 576–606.

Walther, J. V. and Orville, P. M. (1982) Volatile production and transport in regional metamorphism. Contributions to Mineralogy and Petrology, 79, 252–257.

Weill, D. F. and Bottinga, Y. (1970) Thermodynamic analysis of quartz and cristobalite solubilities in water at saturation vapor pressure. Contributions to Mineralogy and Petrology, 25, 125–132.

Weill, D. F. and Fyfe, W. S. (1964) The solubility of quartz in H_2O in the range 1000–4000 bars and 400–500°C. Geochimica et Cosmochimica Acta, 28, 1243–1255.

Wendlandt, H. G. and Glemser, O. (1963) Über die Einwirkung von Wasser auf SiO_2 bei hoheren Drucken und Temperaturen. Naturwissenschaften, 50, 325–353.

Manuscript received, June 18, 1982;
accepted for publication, January 26, 1983.